EXPERIMENTAL RATE COEFFICIENTS FOR COLLISIONAL EXCITATION OF LITHIUM-LIKE IONS*

H.-J. Kunze and W. D. Johnston III

Department of Physics and Astronomy
University of Maryland
College Park, Maryland 20742

UNIVERSITY OF MARYLAND
DEPARTMENT OF PHYSICS AND ASTRONOMY
COLLEGE PARK, MARYLAND

EXPERIMENTAL RATE COEFFICIENTS FOR COLLISIONAL EXCITATION OF LITHIUM-LIKE IONS*

H.-J. Kunze and W. D. Johnston III

Department of Physics and Astronomy
University of Maryland
College Park, Maryland 20742

Collisional excitation rates in N V, O VI and Ne VIII have been derived from absolute line intensities emitted by these ions in a well diagnosed plasma. The plasma was produced in a theta-pinch device, and several plasma conditions were investigated. Electron density and temperature were obtained as a function of radius and time from the spectrum of scattered laser light. The experimental results are compared with Bely's calculations using the Coulomb-Born approximation. Although the accuracy of the individual rate coefficients is a factor of 2 only, the rms deviation of the experimental values from the theoretical ones is about 10% for excitation to the n=2 and n=3 levels and about 15% for excitation to the 4s level. The rates to the 4p and 4d levels are on the average $\sim$60% of the theoretical ones.

---

*Supported by the Atomic Energy Commission.

I. Introduction

Excitation rate coefficients for ions of the lithium isoelectronic sequence are of considerable importance in the spectroscopy of laboratory as well as astrophysical plasmas. In 1963 Heroux[1,2] showed that the intensity ratio of the 2s-2p and 2s-3p transitions in the same Li-like ion allows a unique determination of the electron temperature as long as the plasma is optically thin and collisional depopulation can be neglected. Under these conditions the absolute intensities of the lines are controlled by collisional population rates from the ground state. In the laboratory, this technique has been applied to numerous plasmas. Hinteregger et al.[3] used it to obtain temperatures from solar emission lines. Lines of lithium-like ions are quite prominent in the solar spectrum, and their absolute intensities are conveniently used to deduce relative abundances of the various species[4].

The study of lithium-like ions is further intriguing from a theoretical point of view. Their simple electronic structure renders them amenable to rather detailed calculations (see section II). A comparison of theoretical and experimental data is thus possible.

Direct measurements of the electron impact excitation cross-sections for multiply ionized atoms are very difficult. However, it is quite possible to measure the rate coefficients (i.e. the product of cross-section and initial electron velocity averaged over the electron-velocity distribution function) in transient plasmas[5-9]. Atoms of interest are introduced into a well-diagnosed plasma, and absolute line intensities are then interpreted in terms of desired rate coefficients.

II. Theory

A. Principle of the Measurements

In a plasma which is optically thin with respect to the line radiation of interest the emission coefficient of a spectral line arising from a spontaneous transition between bound levels p and q is given per unit volume and per steradian by

$$\varepsilon(q,p) = \frac{1}{4\pi}\, h\nu(q,p)\, A(q,p)\, N(p)\,, \qquad (1)$$

where $\nu(q,p)$ is the frequency of the emitted radiation, $A(q,p)$ is the atomic transition probability and $N(p)$ is the population density of the upper level. At low electron densities N (i.e. neglecting cascading) the steady-state population[10] of the excited levels is determined by a balance between the sum of collisional excitation rates into that state and the sum of all spontaneous radiative decay rates. Lithium-like ions have the further advantage that they have no metastable levels; at low electron densities excitation occurs thus mainly from the ground state (g), and the emission coefficient may be written

$$\varepsilon(q,p) = \frac{h\nu(q,p)}{4\pi}\, \frac{A(q,p)}{\sum\limits_{r<p} A(r,p)}\, N\, X(p,g)\, N(g)\,, \qquad (2)$$

where $X(p,g)$ is the rate coefficient for excitation from the ground state.

In the actual experiment the determination of the ground state population $N(g)$ of the ion of interest poses a most serious problem. At present there exists no direct way for its determination. The method usually employed, therefore, is to add the atoms of interest in small quantities to the filling gas and to assume that the mixing ratio and composition do not change during the discharge. One further has to know the fraction which is

in the appropriate ionization stage. In steady-state plasmas this fraction can be calculated using the coronal equilibrium relationship. While the distribution of the ions in this model is independent of the electron density, it depends strongly on the magnitude of the collisional ionization and the radiative recombination coefficients. Unfortunately, these are not known with sufficient accuracy. However, in transient hot plasmas the degree of ionization lags behind the corona equilibrium situation: each ion goes through successive ionization stages with a lifetime in each stage determined only by the ionization rates. (Recombination rates are usually very much smaller.) The rate equations governing the population in the various ionization stages are thus very much simplified.

Using the experimentally obtained electron temperature and density time-histories these equations can be solved numerically. It turns out that the peak population in each ionization stage depends less critically on the accurate value of the ionization rates than in the equilibrium situation. Thus estimates of the ground-state populations of the various ions are found with sufficient accuracy. With the emission coefficient $\varepsilon(q,p)$ measured experimentally, Eq. (2) yields then the desired rate coefficient at the temperature existing in the plasma.

B. Theoretical Rate Coefficients for Excitation

Where no specific calculations are available, the cross-sections and rate coefficients for excitation of allowed dipole transitions are usually derived using the well-known $\bar{g}$ approximation of Seaton[11] and Van Regemorter.[12] They used the Bethe-Born approximation in the calculation of the cross-sections, substituted, however, an effective Gaunt factor $\bar{g}$ which they determined empirically from all available cross-section data. In this approximation the rate coefficient can be written

$$X(p,q) = 1.60 \cdot 10^{-5} \frac{f_{pq} \langle\bar{g}\rangle}{\Delta E \sqrt{kT}} \exp\left(-\frac{\Delta E}{kT}\right) \quad [cm^3\ sec^{-1}] \qquad (3)$$

where f_{pq} is the absorption oscillator strength, ΔE the energy difference between levels p and q and kT the electron temperature, both measured in eV. The effective Gaunt factor $\langle\bar{g}\rangle$ averaged over a Maxwellian velocity distribution is given in Ref. 12 and can also be found in Ref. 13. Seaton and Van Regemorter's $\bar{g}$ is a function of $E_i/\Delta E$ only, where E_i is the energy of the incident electrons. When deriving $\bar{g}$ from the quasiclassical line broadening theory [14] suggested an additional dependence on two parameters, namely the Coulomb parameter and the relative size of the dipole matrix elements. This dependence, however, is weak. Work along similar lines has also been done by Roberts[15].

For the collisional excitation by (optically forbidden) monopole or quadrupole transitions, a corresponding approximate formula does not exist. An order of magnitude estimate can be obtained through the collision strength (see, e.g., Refs. 13 and 16).

Recently cross-sections have been calculated specifically for ions of the lithium-isoelectronic sequence. Burke et al.[17] computed the excitation cross-sections corresponding to the array 2s, 2p, 3s, 3p, 3d in NV using both the Coulomb-Born and the close-coupling methods, while Bely[18,19,20] did the calculations for the transitions 2s → ns, 2s → np, and 2s → nd as well as 2p → ns, 2p → np, and 2p → nd for BeII, NV, NeVIII and for a hydrogenic ion with an infinite nuclear charge using only the Coulomb-Born approximation. The conclusions and results of both calculations are essentially the same, where they overlap. Bely's results are given

in a form convenient for extrapolation to other ions and higher principal quantum numbers, so they will be used in the following. He was able to fit the computed cross-sections to an analytical form; this allows a convenient integration over the velocity distribution in order to obtain the rate coefficients. Figure 1 shows these rate coefficients for the excitation from the ground state to the 2p, 3p and 4p levels in NV, OVI and Ne VIII. Figure 2 compares the 2s - 3s, 2s -3p, and 2s -3d excitation rates for NV and Ne VIII. At low electron temperatures (near threshold) the quadrupole and monopole excitation are found to be much larger than the dipole excitation. At higher temperatures all excitation rates are, roughly speaking, comparable, though the quadrupole transition remains the strongest one. According to the author[18,19] the values shown in the curves above should be good to about 20% for the 2s - 2p transitions and to better than 50% for all the other transitions. We should mention, however, that the author calculated the cross-sections only to 5 times and 10 times the threshold energy, respectively, so that the excitation coefficients (Fig. 1 and 2) at high temperatures depend somewhat on the analytical form of the cross-section adopted by Bely,[18] which is correct only for dipole transitions. Further, it is interesting to note that by far the strongest rates in lithium-like ions are those for the 2p - nd transitions.

III. EXPERIMENT

A. Apparatus

The plasma used for these experiments was produced in a Θ-pinch machine described in detail elsewhere.[21] The measurements being discussed were done mainly with an energy of 15 kJ stored in the main bank, although some results were also obtained with the original 9 kJ version. The energy in the preheater was slightly increased; also increased was the damping

of the preheater discharge in order that the main discharge could be fired 15 μsec after the preheater. The filling gas was always hydrogen, and the elements of interest (nitrogen, oxygen and neon) were added in small quantities (<1%). As pointed out in the introduction, one basic assumption for our measurements is that the mixing ratio does not change during the discharge. This assumption is supported by the fact that, when adding known amounts of the impurities, line intensities observed from various ionization stages were found to increase linearly[22], which excludes nonlinear wall effects. The CV 2271 Å line viewed radially at the midplane of the coil was used again as the monitor of the plasma conditions.

Several discharge conditions were investigated. They were obtained by varying the energy stored in the main bank, the filling pressure, the magnitude of the bias magnetic field and the time between the beginning of the preheater discharge and the ignition of the main bank.

B. Determination of Plasma Parameters

The electron density and temperature were derived as a function of radius and time from the analysis of laser light scattered by the plasma. A general description of this technique can be found, e.g., in Ref. 23. The specific setup is identical to that used in Ref. 9, and the whole experimental arrangement can be seen in Fig. 3. Laser head and multichannel detection system are mounted on a common carriage thus permitting easy scanning of the scattering volume along a diameter of the plasma column in the midplane of the coil. Results for two cases are shown in Refs. 9 and 24.

For quantitative spectroscopic observations one needs the length of the hot plasma core. It was determined by observing the CV 2271 Å line through equidistant holes in the coil. The length changed with time, and at the time of maximum compression it varied between 8 and 15 cm for the different discharge conditions.

C. Absolute Sensitivity Calibration of Two Vacuum Ultraviolet Monochromators

The lines of interest from lithium-like ions are in the vacuum-ultraviolet wavelength region. Two monochromators were used for their measurement: a 2-meter grazing incidence instrument (1200 lines per mm and a grazing incidence angle of 86°) covered the wavelength region from 60 Å to 600 Å, while a normal incidence instrument of the Seya-Namioka-type mount was used for the wavelength region above 400 Å.

The most serious problem connected with the measurement of absolute line intensities in the vacuum - UV region is that no reliable radiation standards are available. We employed, therefore, the "branching ratio technique", which was developed by Griffin and McWhirter[25] and by Hinnov and Hofmann.[26] This technique is based on the observation of spectral lines in the vacuum-ultraviolet and in the visible, which originate from the same upper level and are both not affected by self-absorption. The intensity ratio (in photon units) of the two lines is then simply given by the ratio of the respective transition probabilities. The method can be extended to lines which originate from different fine-structure sublevels if one can prove reliably that the sublevels are populated according to their statistical weights.

Both monochromators were equipped with photomultipliers at the exit slit; p-terphenyl as well as the plastic Pilot B were used as scintillators.

The calibration was done in situ, and for this purpose an appropriate plasma was produced in the discharge tube. An aperture stop assured that during both situations, calibration and actual measurement, the field of view of the instruments was limited to 1.5 cm at the center of the discharge tube. During the calibration the same plasma volume was imaged through the other end of the discharge tube onto the entrance slit of a 0.25 meter visible monochromator, also equipped with a photomultiplier tube. This dual arrangement has the advantage that all geometrical factors canceled. The visible instrument was calibrated using both a tungsten lamp and a carbon arc.[27,28]

For the calibration of the grazing incidence instrument the 2s - 3p and 3s - 3p line pairs of lithium-like ions are most suitable. The transition probabilities can be taken from Wiese et. al[29] and should be accurate to within 10%. The intensity ratios of the two lines of the 3s - 3p doublets were found to be 2 in all cases, assuring thus equilibrium population between the two upper levels. The following line pairs were used.

(a) CIV: 312.4Å ($2s^2S_{1/2}$ - $3p^2P_{1/2,3/2}$) and 5802Å ($3s^2S_{1/2}$ - $3p^2P_{3/2}$)

(b) NV: 209.3Å (" ") and 4620Å ($3s^2S_{1/2}$ - $3p^2P_{1/2}$)

(c) OVI: 150.1Å (" ") and 3811Å ($3s^2S_{1/2}$ - $3p^2P_{3/2}$)

(d) NeVIII:[29] 88.1Å (" ") and 2860Å ($3s^2S_{1/2}$ - $3p^2P_{1/2}$)

(e) OV: 172.2Å ($2s^2{}^1S$ - $2s3p\,{}^1P$) and 5114Å ($2s3s\,{}^1S$ - $2s3p\,{}^1P$)

The transition probabilities of the corresponding line pair in beryllium-like OV (e) are much less accurate; however the obtained calibration point falls right on the curve, suggesting that at least the ratio of the transition probabilities is reliable.

The calibration of the Seya-Namioka monochromator was more problematic since not too many suitable line pairs could be found covering the required wavelength region. We finally calibrated the instrument using the following ions and line pairs:

(f) HeII:	1215Å	(n: 2 - 4)	and	4686Å	(n: 3 - 4)
(g) HeII:	1085Å	(n: 2 - 5)	and	3203Å	(n: 3 - 5)
(h) H :	1026Å	(L_β)	and	6563Å	(H_α)
(i) CIII:	574.3Å	($2p\,^1P^o$ - $3d\,^1D$)	and	5696Å	($3p\,^1P^o$ - $3d\,^1D$)
(j) HeI:	515.6Å	($1s\,^1S$ - $5p\,^1P$)	and	3614Å	($2s\,^1S$ - $5p\,^1P$)
(k) HI:	972.5Å	(L_γ)	and	4861Å	(H_β)

In contrast to the calibration of the grazing incidence instrument, where we used the same plasma under investigation also for calibration purposes, we now had to produce different plasmas in the discharge tube, and we will comment on the difficulties encountered for each line pair. The calibration using the HeII line pairs is, in principle, straight forward. For best results we produced a hot plasma with the main bank using an initial filling pressure of 70 mTorr He. However, attention has to be paid to the fact that the strong HeII L_α-line (304Å) in fourth order, as well as spurious amounts of hydrogen (L_α-line) can obscure the HeII line at 1215Å. At 1085 Å we also have the resonance lines of NII; spurious amounts of NII can thus falsify the result. We therefore always cross-checked the NII contribution by comparison with another line at 916Å of the same multiplet.

The L_β - H_α line pair in hydrogen (h) has to be used with caution, because it is nearly impossible to produce a plasma in the laboratory where L_β is not affected by self-absorption, at least in cooler outer regions. The technique usually employed is, therefore,to decrease the density as far as possible and to extrapolate to the absorption free limit.[31] This, however, can still be afflicted with relative large uncertainties, and since it is also difficult to produce plasmas of sufficiently low density in a theta pinch, we modified the method and went to the other extreme. Using a helium-hydrogen mixture (95% helium, 5% hydrogen) at 2 Torr we produced a plasma having an

electron density $N \gtrsim 2 \times 10^{18}$ cm^{-3}. Both lines are now very broad, and their shape is determined by the Stark effect and by self-absorption. The self-absorption, however, affects the line profiles only in the center and not on the wings. Theoretical line profiles for hydrogen are known now to a high accuracy[32,33], and a comparison of the intensities on the wings of the two lines can thus easily be related to the ratio of their total intensities. (Note that the intensity ratio of the wings should be of even higher accuracy than the individual line profiles, since uncertainties in the profiles due to approximations in their calculation will tend to cancel in the ratio).

The CIII line pair poses no experimental problem at low electron densities. Here the drawback is, at present, the large uncertainty in the theoretical transition probabilities.[29] The HeI (j) and H (k) line pairs again will be influenced by self-absorption, since both short wavelength lines go to the ground state. For the L_λ-H_β ratio we used only the preheater discharge, decreased the density as much as possible and extrapolated to zero density; in the case of the HeI line pair we used a hot plasma (10 m Torr He filling pressure) at early times of the discharge. Due to Doppler shift and Doppler broadening the reabsorption of the UV-line in the cooler outer region should be thus decreased.

The calibrations (i) to (k) could be afflicted, as discussed, with relative large uncertainties. A higher degree of accuracy, however, is suggested by the following fact. If we take the known transmission curve of the monochromator[34] and assume constant quantum efficiency for the scintillator (p-terphenyl) , we obtain a relative sensitivity curve which can be scaled to fit the obtained calibration points. The maximum deviation of all six points from this sensitivity curve is found to be 30%, and this covers the wavelength region from 515Å to 1215Å.

D. Experimental Results

Table I shows the emission coefficients of the resonance lines obtained for the different ions under the various discharge conditions. The emission coefficients are given for each line at the time of their peak intensity and are reduced to an impurity concentration of 1% relative to N. (The actual quantity obtained is the intensity of the lines in watt/cm^{2}sr; it was divided by the length of the plasma column.) The $2s^2S - 2p^2P$ transitions of the lithium-like ions pose some difficulties inasmuch as they easily become optically thick. The line intensities were measured, therefore, for various impurity concentrations between 0.1% and 1.0% and were extrapolated, where necessary, to the absorption free limit. There were no problems for NV and NeVIII, and the necessary corrections were usually less than 10%. For OVI, however, the situation was different. Oxygen is a natural contaminant in our plasma. Its concentration varies between 1.5 and 3 percent for the different discharge conditions; the resonance line of OVI was influenced, therefore, by self-absorption already without any addition of oxygen. Although the values obtained are less reliable, attempts were made to correct for the optical thickness theoretically. The resonance lines are broadened only by Doppler effect, and in these cases the optical depth at the center of the line can readily be calculated (see Ref. 32, Eq. 8-14). The temperature of OVI ions was taken to be equal to that of the CV ions. The correction factor for the intensity was obtained similarly as discussed in Ref. 8. Only the value obtained with the lowest electron density is quoted in Table I. The fifth and sixth column give the electron density and temperature (for the same time); the last column, finally, shows the concentrations of the atom in the particular ionization stage obtained by solving the coupled rate equations using a computer program and matching calculated and observed time histories

of spectral lines. Due to changing density and temperature, the time of the peak intensity of a line does not always coincide with that of the peak concentration of the ion.

At low impurity concentrations the two components of the doublet always showed a 2:1 intensity ration, which corresponds to a population of the $2p^2P$ levels according to their statistical weights. For OVI, however, this was not the case any more, the ratio being smaller. This can be understood readily, since the stronger line is much more influenced by self-absorption than the weaker one.

Table II and III give the corresponding results for lines from n = 3 and n = 4 levels, respectively. The fine structure lines were not resolved, so the emission coefficient of the doublet is quoted. We also give the results for one oxygen case only, since at higher electron densities even the $3p \rightarrow 2s$ and $3d \rightarrow 2p$ transitions were influenced by self-absorption.

IV. Interpretation and Discussion

The population densities N(p) of the excited states can be calculated from the measured emission coefficients, using Eq. (1) and the transition probalities as given in Refs. 29 and 35. These are then compared with the total concentration of each ionization stage ($N_{tot} = 10^{-4}pN$ with p given in Tables I to III). The population of the low-lying 2p level is considerable. It varies from ∿7% for Ne VIII to 38% for NV for the highest density case. The total population of all n=3 levels is lower than 0.01% for Ne VIII and around 0.1% for the NV case mentioned above. The total population of all n = 4 levels, finally, is about a factor of 3 below that of the n = 3 levels. In the analysis of the emission coefficients it is justified, therefore, to neglect all ions in higher excited states, i.e., we assume that only the ground and the $2p^2P$ states are significantly populated.

In a first approximation we now make the assumption that the population of the $2p^2P$ level is determined by a balance between collisional excitation from the ground state and radiative decay and collisional de-excitation to the ground state. The de-excitation rate is deduced from the excitation rate using the principle of detailed balance, $X(2p \rightarrow 2s) \approx \frac{1}{3}X(2s \rightarrow 2p)$. The rate coefficients thus obtained are given in Table IV. In order to justify this assumption we consider as a second step also the depopulation of the 2p level by further excitation as well as a population by cascading from higher levels. This results in two additional terms in the rate equation for the population of the 2p level, which we have to compare with each other as well as with the other rates. The cascading contribution is readily obtained from the measured emission coefficients. We consider only cascading from the n = 3 levels, the cascading from the n = 4 levels being found to be smaller by a factor of $\sim$10.

For NeVIII the depopulation by further excitation is found to be about one half the rate for collisional de-excitation to the ground state and only a few percent of the radiative decay rate. (Cross-sections as given by Bely[20] were used for these estimates.) The population of the 2p level by cascading is less than 10% of the collisional excitation rate. Since furthermore both additional rates enter with opposite signs into the rate equation, they tend to cancel, and the total error introduced by neglecting them will be $\sim$5% in this case.

Although $\sim$38% of the NV ions are in the $2p^2P$ state of NV in the high density case, similar results are obtained here. The population of the 2p level by cascading from the n = 3 levels is about 12% of the collisional rate from the ground state; however, this is nearly offset by the strong collisional excitation from the 2p level to all n = 3 levels ($\sim$8% of the total depopulation

rate). The error introduced by neglecting the two additional rates in our simple model will be thus also ∿5% or less. The experimental rates are finally compared with the theoretical rates of Bely[18] and those of Seaton and Van Regemorter.[13]

When considering the population of the n = 3 and n = 4 levels one could neglect cascading; the error being thus introduced is estimated to be ∿20% or less . The situation, however, becomes more complicated inasfar as at higher electron densities not only a strong population via the $2p^2P$ state occurs but also the collisional rates between levels of the same principal quantum number become comparable or even larger than the radiative rates: the levels would be populated then according to their statistical weights and no individual excitation rates can be deduced any more.

We consider first the high-density NV case. The cross-sections for collisional transitions between the n = 3 levels have been calculated by Burke et al.[17] We compare now the collisional rates with the radiative transition probabilities.[29]

$$\frac{NX(3p \rightarrow 3s)}{A(3p \rightarrow 2s)} \approx 0.06; \qquad \frac{NX(3p \rightarrow 3d)}{A(3p \rightarrow 2s)} \approx 0.12$$

$$\frac{NX(3s \rightarrow 3p)}{A(3s \rightarrow 2p)} \approx 0.22 \qquad \frac{NX(3d \rightarrow 3p)}{A(3d \rightarrow 2p)} \approx 0.02$$

The population densities are obtained from the measured emission coefficients: $N(3s) = 0.85 \times 10^{10}$; $N(3p) = 1.37 \times 10^{10}$; $N(3d) = 1.02 \times 10^{10}\ cm^{-3}$.

The level most severely influenced by n = 3 collisional transitions is the 3s level, the 3s → 3p transition being 22% of the radiative decay. More than one half of this population loss, however, is offset by collisional transitions in the opposite direction, so that the net drain of the 3s level by collisions to the 3p level is about 10% only. Similarly, the population of the 3d level occurs to about 10% through collisions from the 3p level. The population of the 3p level is practically not influenced by these collisions, the drain to the 3d level being nearly offset by the gain from the 3s level. For the lower electron densities the collisions between the n = 3 levels become even less important. Naturally they can be neglected for the higher Z ions O VI and Ne VIII in our cases.

Serious, however, is the excitation of the n = 3 levels via the 2p level. We consider again, at first, the high-density N V case (T_e = 110 eV, N = 6.2 x 10^{15} cm^{-3}). Theoretical calculations[18,19,20] yield

$$X\ (2s \rightarrow 3s) = 7.1 \times 10^{-10}\ ;\quad X\ (2p \rightarrow 3s) = 1.6 \times 10^{-10}$$

$$X\ (2s \rightarrow 3p) = 5.6 \times 10^{-10}\ ;\quad X\ (2p \rightarrow 3p) = 10.6 \times 10^{-10}$$

$$X\ (2s \rightarrow 3d) = 14.8 \times 10^{-10};\quad X\ (2p \rightarrow 3d) = 49.4 \times 10^{-10}$$

and from the experiment one obtains

$$N\ (2s) = 1.78 \times 10^{13}\ ;\quad N\ (2p) = 1.07 \times 10^{13} cm^{-3}.$$

Theoretically one obtains thus in this case that the population via the 2p level is 13% for the 3s level, 53% for the 3p level and even

67% for the 3d level. (The corresponding values for Ne VIII, T_e = 260 eV, N = 4.5 x 10^{15} cm^{-3}, are 1%, 8% and 18% respectively). For all cases and ions it is thus possible to derive the 2s → 3s excitation rate directly from the corresponding emission coefficient; this also still possible (with a small correction) for the rates to the 3p and 3d levels of Ne VIII. However for N V one obtains for 3p and 3d only rates averaged over the 2s and 2p levels.

For all theoretical excitation cross-sections the Coulomb-Born approximation was used.[18,19,20] Since our average kinetic energies are at least 3 times above threshold, the relative magnitude of the cross-sections from the 2s and 2p levels should be very reliable, even if the absolute values show larger uncertainties; approximations should influence both cross-sections in the same way and will tend to cancel in the ratio. We accept, therefore, the theoretical ratio of the excitation rates (which is a function of T) and use it in the analysis of the data. Table V shows the emission coefficients thus obtained. They again are compared with theoretical values. (For O VI the population of the 2p level was calculated using the theoretical rate since the resonance line was optically thick.)

In the final evaluation of the rate coefficients also the cascading contributions from the n = 4 levels were taken into account, since they could be derived from measured line intensities. (For N V they were, for example, 4% for the 3s level, 7% for the 3p level and ∿7% for the 3d level, where the cascading from the 4f level could be estimated only.)

Collisions within the n = 4 levels will influence the respective population densities more severely than within the n = 3 levels. No theoretical calculations are available at present. Classical scaling suggests that the rates are larger by a factor of ∿3 compared to those within the n = 3 levels. Since the radiative rates are smaller by a factor ∿2, the ratios of collisional n = 4 transitions to radiative decay rates are larger by a factor of about 6 as compared to the respective ratios for the n = 3 levels. Individual excitation rates could thus be off by up to 50% as in the high-density N V case. However, these collisions still do not dominate the population densities, which can be seen from the experimentally obtained values. In the collision-dominated case one would find N(4s):N(4p):N(4d) = 1:3:5. Table VI shows the rate coefficients derived. A 10% correction for cascading was applied in all cases.

The maximum error for the individual rate coefficients is estimated to be a factor of 2 for excitation to the n = 2 and n = 3 levels, and better than a factor of 2.5 for excitation to the n = 4 levels. The errors could be somewhat larger for O VI due to some optical depth effect as well as due to a possible systematic error in determining the impurity concentration, since oxygen is a natural contaminant with relatively large concentrations in our plasmas.

V. Summary

Excitation rate coefficients for lithium-like ions are derived from absolute line intensities emitted by suitable ions in well-diagnosed plasmas. The results are compared with calculations using the Coulomb-Born approximation.

Although the experimental errors are inherently large (a factor $\sim$2), the individual agreement is remarkable in many cases. If one claculates the rms deviation of the experimental values from the theoretical ones averaged over N V, O VI and Ne VIII, one obtains a deviation of only $\sim$10% for excitation to the n = 2 and n = 3 levels and $\sim$15% for excitation to the 4s level. The rates for excitation to the 4p and 4d levels, however, are consistently about 40% below the theoretical ones. This large discrepancy cannot be caused by further excitation or ionization. The ionization rate is estimated[24], for example, to be less than 3% of the radiative decay rate.

After completion of this work a paper by Boland et al.[36] appeared on measurements of excitation rates for NV at one temperature (20eV). The results were found to agree with theory within the experimental accuracy of 50%.

VI. Acknowledgements

The authors would like to express their appreciation to H. R. Griem for valuable discussions. The computer time for this project was supported by the National Aeronautics and Space Administration Grant NSG-398 to the Computer Science Center of the University of Maryland. The National Science Foundation, gave a grant for the purchase of the grazing incidence spectrograph used in this work.

REFERENCES

1. L. Heroux, Nature, Lond., 198, 1291 (1963).
2. L. Heroux, Proc. Phys. Soc., 83, 121 (1964).
3. H. E. Hinteregger, L. A. Hall, and W. Schweizer, Astrophys. J., 140, 319 (1964).
4. K. G. Widing and G. D. Sandlin, Astrophys. J. 152, 545 (1968).
5. B. Boland, F. Jahoda, T. J. L. Jones, and R. W. P. McWhirter, Proceedings of the Fourth International Conference on the Physics of Electronic and Atomic Collisions, Quebec, 1965, edited by L. Kerwin and W. Fite (Science Bookcrafters, Hastings-on-Hudson, N. Y., 1965).
6. E. Hinnov, J. Opt. Soc. Am., 56, 1179 (1966) and 57, 1392 (1967).
7. L. C. Johnson, Phys. Rev. 155, 64 (1967).
8. R. C. Elton and W. W. Köppendörfer, Phys. Rev. 160, 194 (1967).
9. H.-J. Kunze, A. H. Gabriel and H. R. Griem, Phys. Rev. 165, 267 (1968).
10. The assumption of a steady-state population for the excited states is justified in all practical cases. Characteristic times for changes in the excited-state densities are of the order of radiative lifetimes A^{-1}, see Ref. 9.
11. M. J. Seaton, in Atomic and Molecular Processes, edited by D. R. Bates (Academic Press Inc., New York 1962), p. 414,
12. H. Van Regemorter, Astrophys. J., 136, 906 (1962).
13. C. W. Allen, Astrophysical Quantities, Second Edition, The Athlone Press, University of London, 1963.
14. H. R. Griem, Phys. Rev. 165, 258 (1968).

15. D. E. Roberts, Sixth Internaltional Conference on the Physics of Electronic and Atomic Collisions, Cambridge, Mass., Abstracts of Papers, MIT Press, 1969, p. 257.

16. R. C. Elton, in Methods of Experimental Physics - Plasma Physics, edited by H. R. Griem and R. H. Lovberg, (Academic Press Inc., New York, 1970).

17. P. G. Burke, J. H. Tait and B. A. Lewis, Proc. Phys. Soc. 87, 209 (1966).

18. O. Bely, Proc. Phys. Soc. 88, 587 (1966) and Ann. d'Astrophys. 29, 131 (1966).

19. O. Bely, Ann. d'Astrophys. 29, 683 (1966).

20. O. Bely and D. Petrini, Astron. and Astrophys. 6, 318 (1970).

21. A. W. DeSilva and H.-J. Kunze, J. Appl. Phys. 39, 2458 (1968).

22. H.-J. Kunze and A. H. Gabriel, Phys. Fluids 11, 1216 (1968).

23. H.-J. Kunze, in Plasma Diagnostics, edited by Lochte-Holtgreven (North Holland Publishing Co., Amsterdam, 1968).

24. H.-J. Kunze, to be published.

25. W. C. Griffin and R. W. P. McWhirter, Proc. Conf. Optical Instruments and Techniques (London, Chapman and Hall, 1962) p. 14.

26. E. Hinnov and F. W. Hofmann, J. Opt. Soc. Am. 53, 1259 (1962).

27. H. Magdeburg, Z. Naturforsch. 20a, 980 (1965).

28. A. T. Hattenburg, Appl. Opt. 6, 95 (1967).

29. W. L. Wiese, M. W. Smith, and B. M. Glennon, National Bureau of Standards. Report No. NSRDS-NBS-4, Vol. 1, 1966.

30. W. D. Johnston III and H.-J. Kunze, Astrophys. J. 157, 1469 (1969).

31. J. L. Schwob, Thesis, Faculte des Sciences de Paris, France, 1967.

32. H. R. Griem, Plasma Spectroscopy (McGraw-Hill Book, Co., New York, 1964).

33. P. Kepple and H. R. Griem, Phys. Rev. 173, 317 (1968).

34. We thank J. R. Greig for supplying the transmission curve for the Seya-Namioka monochromator. It was obtained by using two instruments in tandem.

35. B. Warner, Mon. Not. Roy. Astr. Soc. 141, 273 (1968).

36. B. C. Boland, F. C. Jahoda, T. J. L. Jones and R. W. P. McWhirter, J. Phys. B: Atom. Molec. Phys. 3, 1134 (1970).

FIGURE CAPTIONS

Fig. 1. Excitation rate coefficients after Bely as a function of electron temperature for the transitions $2s \rightarrow np$ with $n = 2,3,4$ in N V, O VI and Ne VIII.

Fig. 2. Excitation rate coefficients after Bely as a function of electron temperature for the transitions $2s \rightarrow 3\ell$ with $\ell = s,p,d$ in N V and Ne VIII.

Fig. 3. Experimental arrangement.

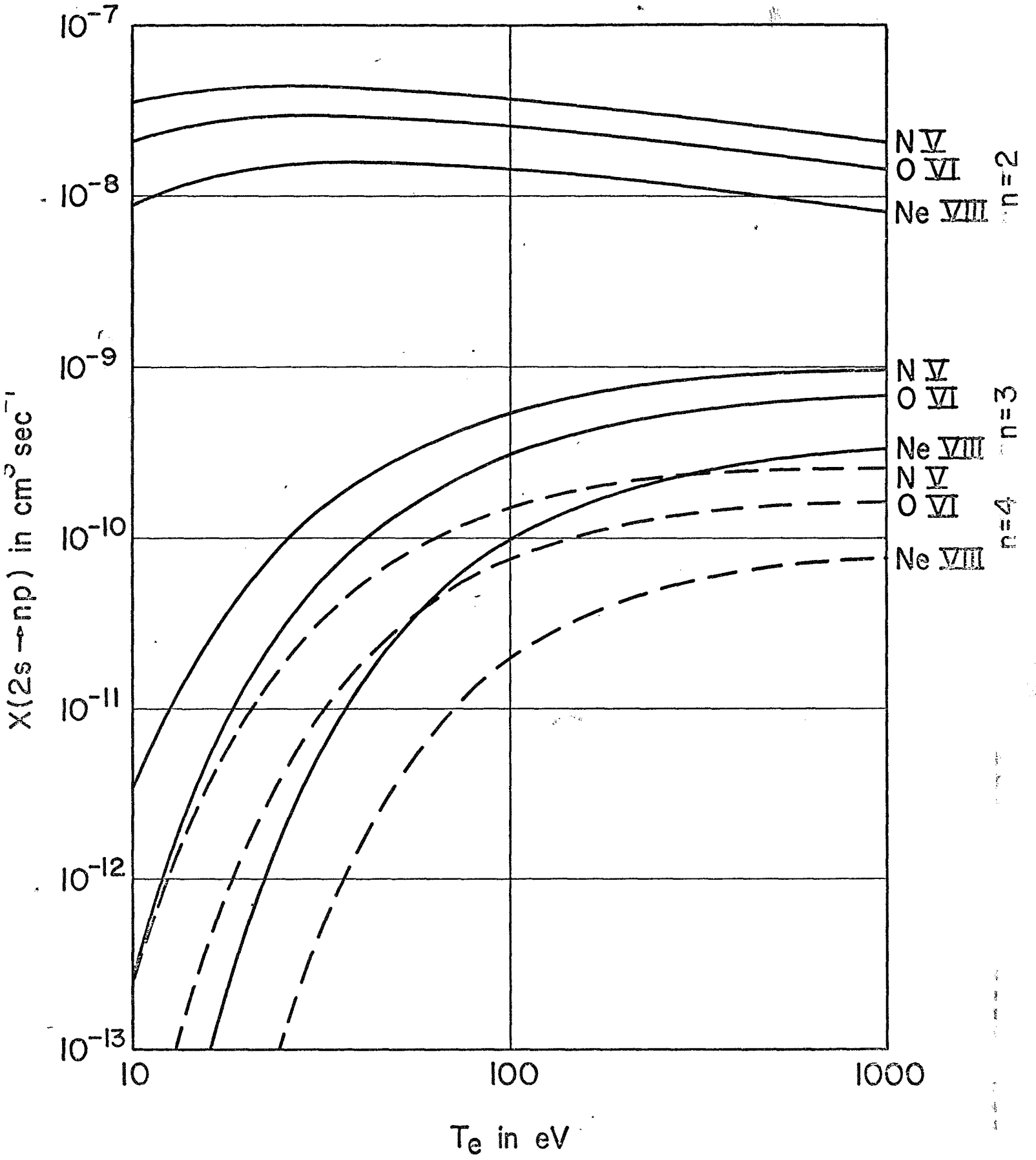
10^{-7}
10^{-8}
10^{-9}
10^{-10}
10^{-11}
10^{-12}
10^{-13}
$X(2s \rightarrow np)$ in $cm^3 sec^{-1}$
10
100
1000
T_e in eV
N V
O VI
Ne VIII
n=2
N V
O VI
Ne VIII
n=3
N V
O VI
Ne VIII
n=4

Fig. 1

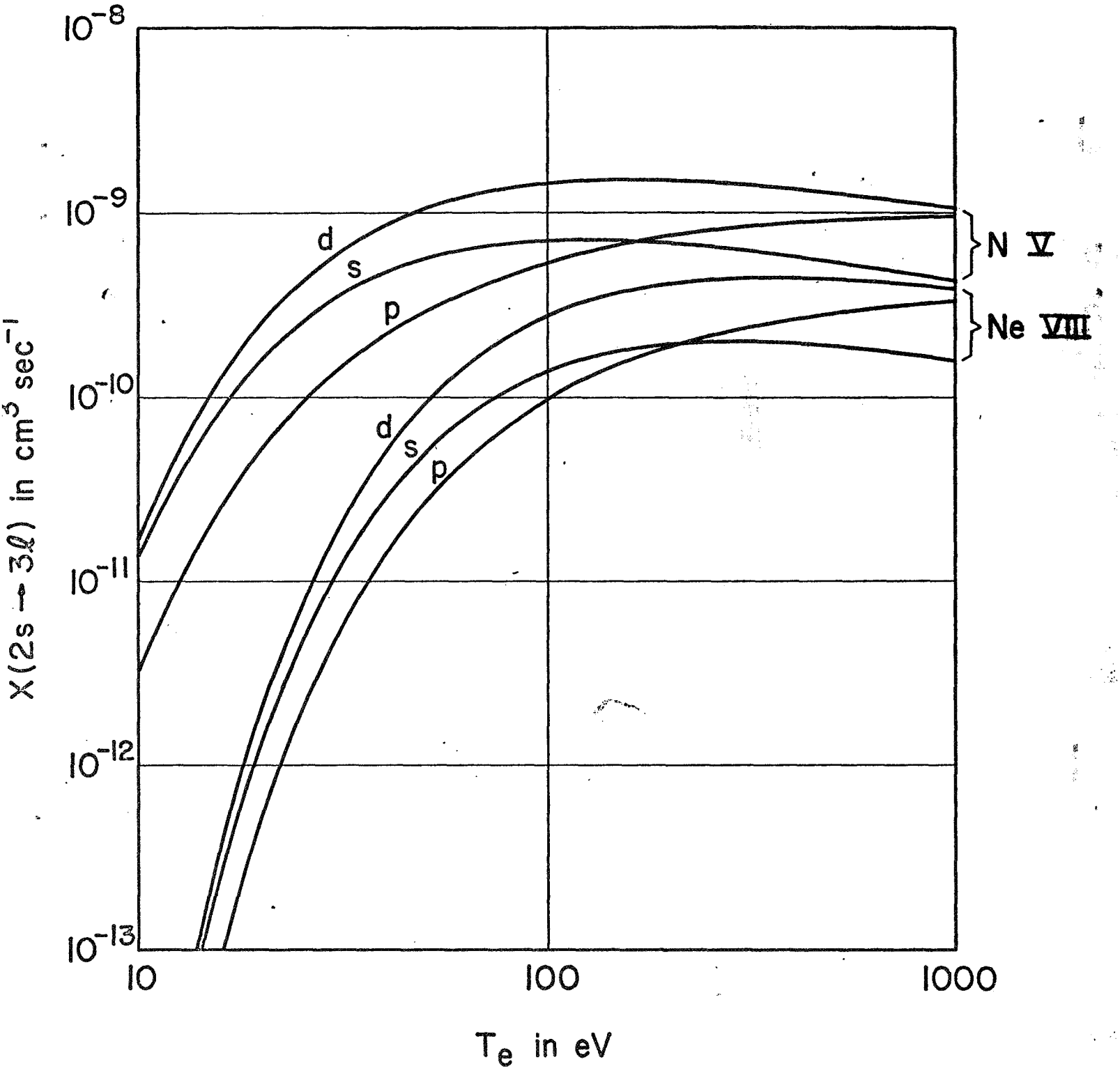
10^{-8}
10^{-9}
10^{-10}
10^{-11}
10^{-12}
10^{-13}
$X(2s \rightarrow 3\ell)$ in $cm^3\ sec^{-1}$
d
s
p
d
s
p
N V
Ne VIII
10
100
1000
T_e in eV

Fig.

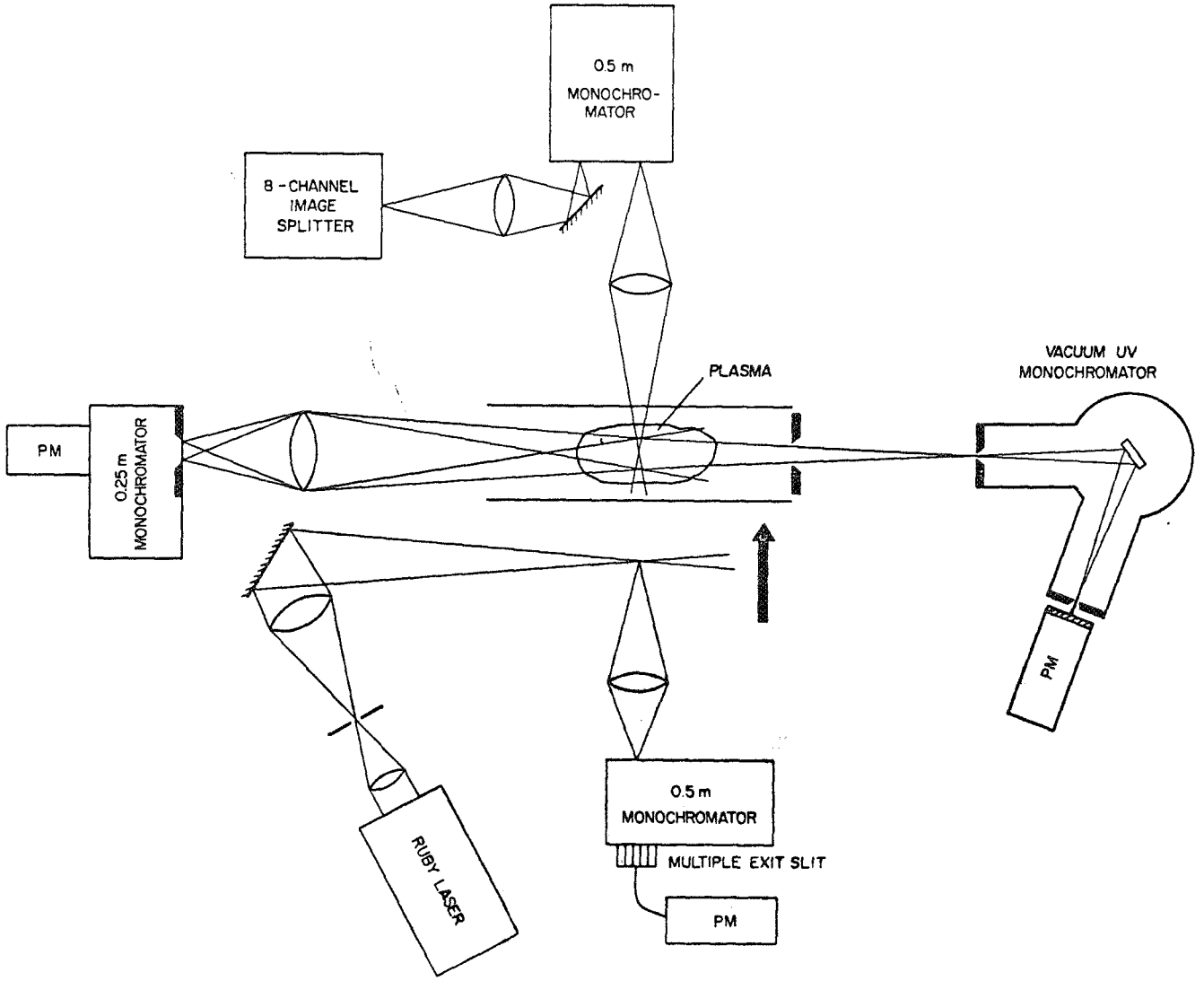
0.5 m
MONOCHRO-
MATOR
8 - CHANNEL
IMAGE
SPLITTER
PLASMA
VACUUM UV
MONOCHROMATOR
PM
0.25 m
MONOCHROMATOR
PM
RUBY LASER
0.5 m
MONOCHROMATOR
MULTIPLE EXIT SLIT
PM

Fig. 3

Table I. $2s\ ^2S - 2p\ ^2P$ radiative transitions

Ion	Transition	λ in A^o	ε in W/cm^2sr	N in cm^3	T in eV	p in %
Ne VIII	$2s^2S-2p^2P_{3/2}$	770.4	112	4.5×10^{15}	260	46
			197	6.4×10^{15}	165	55
			236	6.9×10^{15}	125	56
O VI	$2s^2S-2p^2P_{3/2}$	1032	73	2.8×10^{15}	215	45
N V	$2s^2S-2p^2P_{1/2,3/2}$	1240	185	3.8×10^{15}	210	44
			306	4.9×10^{15}	145	44
			460	6.2×10^{15}	110	46
			118	2.8×10^{15}	215	44

Table II. Radiative transitions from n = 3 levels

Ion	ε in W/cm^2sr			N in cm^3	T in eV	p in %
	2s - 3p	2p - 3s	2p - 3d			
Ne VIII	37	28	64	4.5×10^{15}	260	46
	75	53	151	6.4×10^{15}	165	55
	118	81	183	6.9×10^{15}	125	56
O VI	30	24	87	5.0×10^{15}	260	45
N V	45	22	87	3.8×10^{15}	210	44
	75	32	165	4.9×10^{15}	145	44
	124	46	279	6.2×10^{15}	110	46

Table III. Radiative transitions from n = 4 levels

Ion	ε in W/cm^2sr			N in cm^3	T in eV	p in %
	2s - 4p	2p - 4s	2p - 4d			
Ne VIII	6.5	4.2	7.4	4.5×10^{15}	260	46
	8.2	11.0	13.5	6.4×10^{15}	165	55
	13.5	12.8	20.4	6.9×10^{15}	125	56
O VI	6.4	2.5	9.2	5.0×10^{15}	260	45
N V	4.6	2.8	13.8	3.8×10^{15}	210	44
	7.7	4.6	19.4	4.9×10^{15}	145	44
	10.9	5.3	33	6.2×10^{15}	110	46

Table IV. 2s → 2p Excitation Rate Coefficients

Ion	T in eV	X(2s → 2p)		
		measured	Bely	Seaton, v. Regemorter
Ne VIII	260	1.0×10^{-8}	1.2×10^{-8}	0.6×10^{-8}
	165	0.7×10^{-8}	1.3×10^{-8}	0.6×10^{-8}
	125	0.7×10^{-8}	1.4×10^{-8}	0.6×10^{-8}
O VI	215	2.5×10^{-8}	2.2×10^{-8}	1.2×10^{-8}
N V	215	3.8×10^{-8}	3.1×10^{-8}	1.8×10^{-8}
	210	3.6×10^{-8}	3.2×10^{-8}	1.8×10^{-8}
	145	4.0×10^{-8}	3.4×10^{-8}	1.9×10^{-8}
	110	4.1×10^{-8}	3.7×10^{-8}	1.9×10^{-8}

Table V. Excitation Rates to n = 3 Levels

Ion	Rate Coefficient	T in eV	Measured	Bely
Ne VIII	X(2s → 3s)	125	1.9×10^{-10}	1.6×10^{-10}
		165	1.6×10^{-10}	1.9×10^{-10}
		260	2.0×10^{-10}	2.0×10^{-10}
	X(2s → 3p)	125	2.0×10^{-10}	1.3×10^{-10}
		165	1.5×10^{-10}	1.6×10^{-10}
		260	1.9×10^{-10}	2.2×10^{-10}
	X(2s → 3d)	125	3.4×10^{-10}	3.3×10^{-10}
		165	3.5×10^{-10}	4.0×10^{-10}
		260	3.4×10^{-10}	4.4×10^{-10}
O VI	X(2s → 3s)	260	3.0×10^{-10}	4.3×10^{-10}
	X(2s → 3p) = 0.94X(2p → 3p)	260	2.5×10^{-10}	5.2×10^{-10}
	X(2s → 3d) = 0.33X(2p → 3d)	260	5.3×10^{-10}	9.5×10^{-10}
N V	X(2s → 3s)	110	6.6×10^{-10}	7.1×10^{-10}
		145	6.7×10^{-10}	7.1×10^{-10}
		210	7.6×10^{-10}	6.8×10^{-10}
	X(2s → 3p) = 0.53X(2p → 3p)	110	6.3×10^{-10}	5.6×10^{-10}
	= 0.64X(2p → 3p)	145	7.0×10^{-10}	6.5×10^{-10}
	= 0.79X(2p → 3p)	210	7.7×10^{-10}	7.5×10^{-10}
	X(2s → 3d) = 0.30X(2p → 3d)	110	1.2×10^{-9}	1.5×10^{-9}
	= 0.30X(2p → 3d)	145	1.3×10^{-9}	1.5×10^{-9}
	= 0.29X(2p → 3d)	210	1.2×10^{-9}	1.5×10^{-9}

Table VI. Excitation rates to n = 4 levels

Ion	Rate Coefficient	T in eV	Measured	Bely
Ne VIII	X(2s → 4s)	125	3.7×10^{-11}	2.3×10^{-11}
		165	3.7×10^{-11}	2.8×10^{-11}
		260	3.5×10^{-11}	3.4×10^{-11}
	X(2s → 4p)	125	2.5×10^{-11}	2.7×10^{-11}
		165	2.0×10^{-11}	3.7×10^{-11}
		260	3.5×10^{-11}	5.2×10^{-11}
	X (2s → 4d)	125	3.5×10^{-11}	4.2×10^{-11}
		165	2.8×10^{-11}	5.3×10^{-11}
		260	4.0×10^{-11}	6.6×10^{-11}
O VI	X(2s → 4s)	260	3.3×10^{-11}	7.5×10^{-11}
	X(2s → 4p) = X(2p → 4p)	260	5.2×10^{-11}	13×10^{-11}
	X(2s → 4d) = 0.32X(2p → 4d)	260	5.5×10^{-11}	16×10^{-11}
N V	X(2s → 4s)	110	0.8×10^{-10}	1.2×10^{-10}
		145	1.1×10^{-10}	1.2×10^{-10}
		210	1.0×10^{-10}	1.2×10^{-10}
	X(2s → 4p) = 0.68X(2p → 4p)	110	0.63×10^{-10}	1.6×10^{-10}
	= 0.78X(2p → 4p)	145	0.8×10^{-10}	1.9×10^{-10}
	= 0.95X(2p → 4p)	210	0.9×10^{-10}	2.2×10^{-10}
	X(2s → 4d) = 0.33X(2p → 4d)	110	1.5×10^{-10}	2.4×10^{-10}
	= 0.32X(2p → 4d)	145	1.5×10^{-10}	2.5×10^{-10}
	= 0.31X(2p → 4d)	210	2.0×10^{-10}	2.6×10^{-10}